Contrib. Astron. Obs. Skalnaté Pleso **44**, 5 – 18, (2014)

The accumulations of solids beyond the primordial Jupiter and Saturn to form the ice-giant cores

M. Jakubík and L. Neslušan

Astronomical Institute of the Slovak Academy of Sciences
059 60 Tatranská Lomnica, The Slovak Republic, (E-mail: mjakubik@ta3.sk; ne@ta3.sk)

Received: July 8, 2013; Accepted: February 17, 2014

Abstract. We study the dynamics of small bodies in the dissipating solar nebula during the era when Jupiter and Saturn were already formed and occupied mutual 3:2 mean-motion resonance. The study is done in the course to reveal the eventual sites of accumulation of material in the proto-planetary disk. Such an accumulation could significantly enhance the formation of the ice-giant cores. Actually, we found that the resonant action of Jupiter and Saturn in combination with the gas drag of the dissipating solar nebula may create two maxima in the distribution of solid material beyond Saturn, if the prevailing amount of the solids is concentrated in kilometer-sized or smaller bodies. Specifically, the distribution is then peaked at about ~ 11 and ~ 16.5 AU. A higher amount of solid material is in smaller bodies, the higher peaks occur. We suspect that the two maxima correspond to just two existing ice giants, Uranus and Neptune.

Key words: giant planet formation – Uranus – Neptune

1. Introduction

Although the basic features of the Solar System formation are well known, some details of the formation scenario still remain to be specified. We know that a fragment of an interstellar cloud collapsed into the proto-sun and circumambient gaseous solar nebula. Inside the nebula, the macroscopic planetesimals were created and accreted into the planets. The accretion of the outer giant planets happened earlier than the accretion of inner terrestrial planets.

The giant planets had to accrete in two stages. The formation of gas giants, Jupiter and Saturn, had to be more or less completed before the gaseous nebula dissipated. Otherwise, these planets could not contain their massive atmospheres consisting mostly of hydrogen and helium. On the other hand, the ice giants, Uranus and Neptune, had to accrete later, in a solid-objects-dominating environment.

Many details of the Uranus and Neptune formation are not known. In our work we try to specify the most probable accretion sites of these planets. Obvi-

ously, the dusty grains and comet sized bodies (which we will refer as ,,solid material", hereinafter) were not longer distributed smoothly in the proto-planetary disc (PPD, hereinafter) after the formation of Jupiter and Saturn due to their gravitational perturbations. The highest concentration of the solid material could be expected especially in the resonances with them.

In addition, we do not see any serious reason to postpone the beginning of the Uranus and Neptune accretion process after the complete dissipation of the solar nebula. On the contrary, the gas drag of the nebula at the end of its existence could significantly enhance the accretion process. We therefore consider the weaker and weaker gas drag of the gradually disappearing gaseous nebula.

The recent version of the Nice model (Tsiganis *et al.*, 2005) of the final stage of giant-planet formation predicted the important feature of the formation process: Jupiter and Saturn most likely occupied their mutual 3:2 mean-motion resonance (MMR, hereinafter) in an early era of their existence (Masset and Snellgrove, 2001; Morbidelli and Crida, 2007). Consequently, it seems to be reasonable to consider this configuration at the beginning of the ice-giants formation.

In this work, we study the dynamics of small bodies in the dissipating solar nebula during the era when Jupiter and Saturn were already formed and occupied mutual 3:2 MMR in the course to reveal some eventual sites of accumulation of material (e.g. the MMRs, especially with Saturn), which could significantly enhance the formation of the ice-giant cores. The capture of bodies in the outer MMRs by the giant planets also protected them to spiral inward and come closely to Saturn and Jupiter.

2. The dynamical evolution of small bodies in the dissipating solar nebula

In the era immediately after the Jupiter and Saturn were formed, these planets revolved around the Sun in almost co-planar and circular orbits near their 3:2 MMR, at the heliocentric distances equal to 5.45 and 7.41 AU, respectively. At that time, the PPD was obviously dynamically evolved enough. For the sake of simplicity, we nevertheless consider a smooth initial distribution of small bodies in the PPD, with the initial surface-density profile of a dust component proportional to $\propto r^{-3/2}$ (Hayashi, 1981). In more detail, we consider 4946 test particles (TPs, hereinafter) of a given size and mean density in the interval of heliocentric distances from 3 to 35 AU. The small bodies initially situated in the terrestrial-planet region ($r < 3$ AU) obviously did not cross the orbits of gas giants and contributed to the formation of Uranus and Neptune. On the contrary, very distant small bodies could spiral toward the Sun. Some tests, however, showed that the bodies initially situated beyond 35 AU certainly could not move to the Uranus-Neptune formation region (within $\sim$20 AU from the

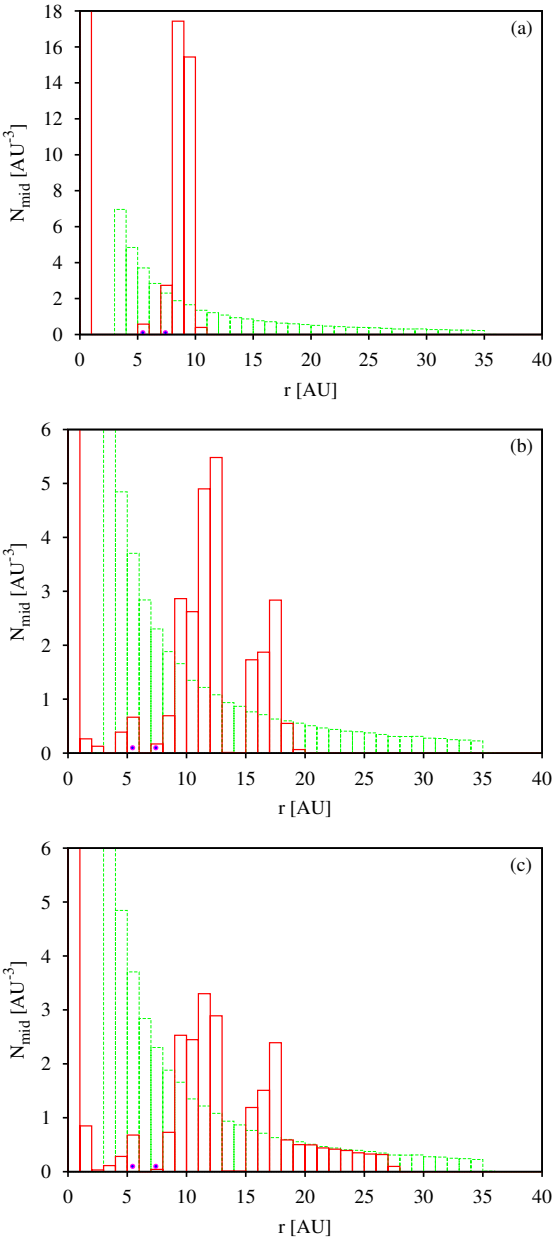

Figure 1. – 1-st part; figure continues on the next page.

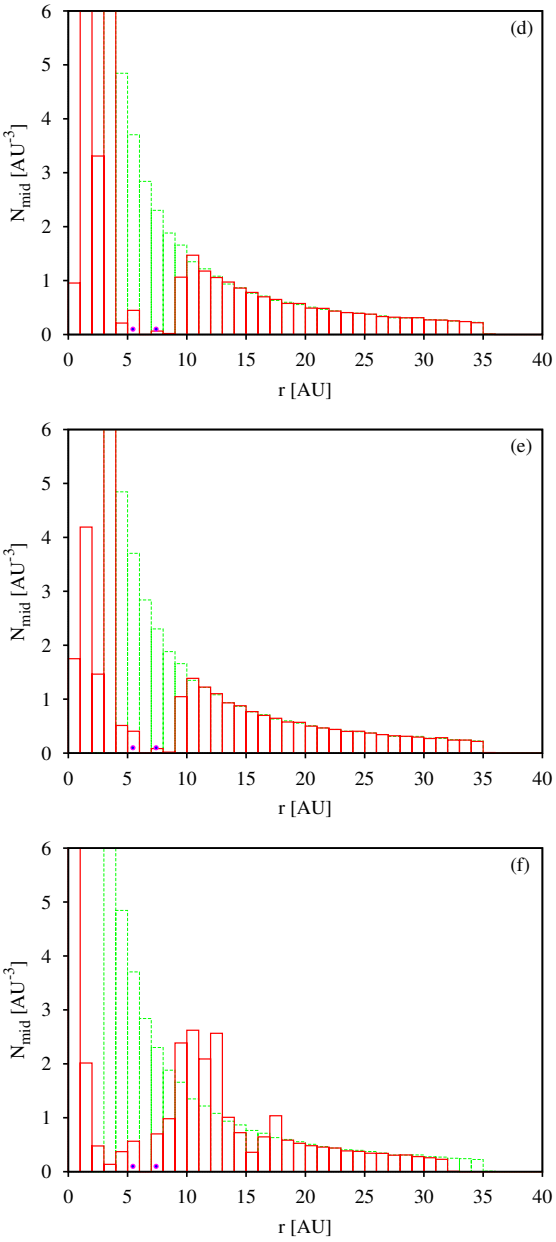

Figure 1. – 2-nd part; figure started on the previous and continues on the next page.

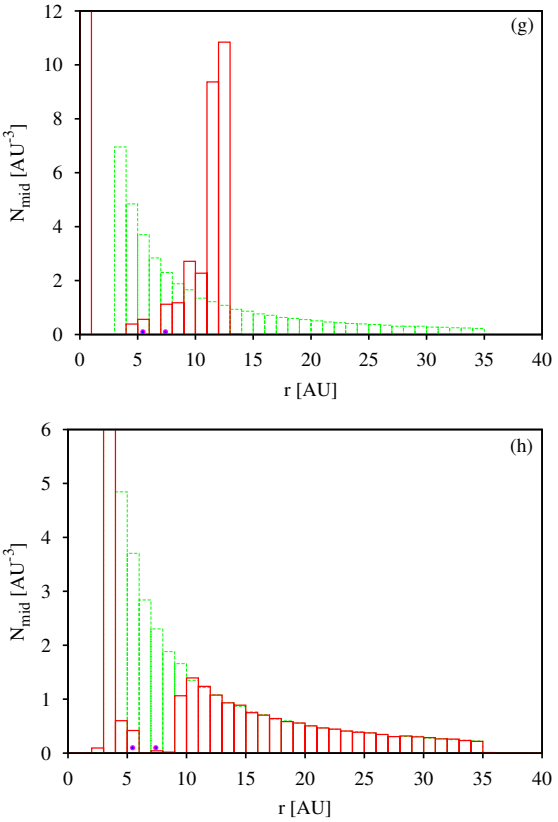

Figure 1. – 3-rd part; the 1-st and 2-nd parts are on previous pages. The mid-plane number surface density in 20 Myr as yielded from the performed runs of the study of TP dynamical evolution (see the text of Sect. 2 for the description of runs and further context; denotation of the plots coincides with that of the runs). The mid-plane number surface density gives the number of TPs, N_{mid}, within the given interval (bar) of heliocentric distance, r, which are at a distance from the invariable plane of the given planetary system smaller than 1 AU. N_{mid} in 20 Myr is shown with the solid (red) bars, the initial N_{mid} with dashed (green) bars. The initial heliocentric distances of Jupiter (5.45 AU) and Saturn (7.41 AU) are illustrated by full circles. Notice the different vertical scales of plots (a) and (g).

Sun) during the considered evolutionary period of 20 Myr. The initial orbits of TPs are almost circular and co-planar. The distributions of eccentricity and inclination to the Jupiter-Saturn invariable plane are described with the half-Gaussians centred at zero with the dispersions of 0.01 and 0.01 rad, respectively.

Jupiter, Saturn and all TPs considered are embedded inside the gaseous solar nebula. The latter was already highly evolved. To respect this circumstance, we consider the gas density profile, when calculating the gas drag, from the hydrodynamical simulations of Morbidelli and Crida (2007). The dynamical evolution of the TPs is followed via numerical integration of their orbits, whereby we utilize the SyMBA, version 5, software package (Duncan *et al.*, 1998). The standard SyMBA gas-drag subroutine is modified to comprehend the dissipation of the gas by setting the simple decay law $\exp(-t/\tau)$, where t is time and τ is $\exp(-1)$-decay time. We use the nominal value of $\tau = 5\,\mathrm{Myr}$ implying a longer dissipation time. Such longer time can be justified by the recent conclusion in work by Machida et al. (2010) that, in the standard model they considered, the growth timescale of the planetary core is 2.7×10^7 yr at the Jovian orbit and 1.7×10^8 yr at the Saturnian orbit. It means that the gaseous solar nebula had to persist for at least a few ten million years so that the cores of Jupiter and Saturn could form.

The proper computation is performed using the GRID computational system of a number of independently working CPUs. In more detail, we use 100 CPUs for each computation. Using of this system is possible, here, since the characteristics of a given TP do not depend on the characteristics of any other TP during the entire integration. The computation of mutually depending characteristics of Jupiter and Saturn is repeated by every CPU.

The effect of the gas drag is selective, depending on the size (cross-section) and mean density of the object. In our study of the TP dynamics, we therefore perform several runs considering the following values of the radius, R_{tp}, and the mean density, ρ_{tp}, of the TPs:
(a) $R_{tp} = 0.1\,\mathrm{km}$, $\rho_{tp} = 500\,\mathrm{kg\,m^{-3}}$;
(b) $R_{tp} = 1\,\mathrm{km}$, $\rho_{tp} = 500\,\mathrm{kg\,m^{-3}}$;
(c) $R_{tp} = 10\,\mathrm{km}$, $\rho_{tp} = 1000\,\mathrm{kg\,m^{-3}}$;
(d) $R_{tp} = 100\,\mathrm{km}$, $\rho_{tp} = 2000\,\mathrm{kg\,m^{-3}}$;
(e) $R_{tp} = 1000\,\mathrm{km}$, $\rho_{tp} = 2000\,\mathrm{kg\,m^{-3}}$.
In addition, we perform the run with a more rapid nebula dissipation with $\tau = 1\,\mathrm{Myr}$ for
(f) $R_{tp} = 1\,\mathrm{km}$, $\rho_{tp} = 500\,\mathrm{kg\,m^{-3}}$,
as well as the run with no dissipation, again for
(g) $R_{tp} = 1\,\mathrm{km}$, $\rho_{tp} = 500\,\mathrm{kg\,m^{-3}}$,
and, finally, we also perform a checking run for
(h) the TPs in a free space, with no gas drag.

We follow the dynamics of the TPs for a 20 Myr period. After this time, the gas of the solar nebula is largely gone even in the case of the lower dissipation rate, $\tau = 5\,\mathrm{Myr}$.

To find the most appropriate sites of the accretion of Uranus and Neptune, we define the *mid-plane number surface density*, N_{mid}. It gives the number of TPs in the volume between the radii r and $r + dr$ at the distance from the invariable plane of a given planet system smaller than 1 AU (in contrast to the common number surface density giving this number from minus infinity to plus infinity distance from the mid-plane). The resultant N_{mid}, for the individual runs in the final time of 20 Myr, is shown in Fig. 1.

Table 1. The semi-major axes (in AU) of the orbits, in two regions of our interest, corresponding to several outer mean-motion resonances (MMRs) with Jupiter and Saturn in the configuration considered.

MMR	with Jupiter	with Saturn
5 : 7		9.1
2 : 3		9.6
5 : 8		10.0
3 : 5		10.3
4 : 7		10.6
5 : 9		10.8
1 : 2		11.6
4 : 9	9.3	12.5
3 : 7	9.5	12.8
2 : 5	10.0	
3 : 8	10.4	
1 : 3	11.3	15.2
2 : 7	12.5	16.8
1 : 5	15.9	
1 : 6	17.9	

Looking at this figure, we can see an important dependence of the accumulation of matter, in our context of ice-giant accretion, on the dissipation rate. In the case of moderate dissipation, with $\tau = 5$ Myr, the TPs with radii 1 and 10 km are concentrated, beyond the orbit of Saturn, into two regions being at the distances 9−13 and 15−18 AU (Fig. 1b, c). For $R_{tp} = 1$ km ($R_{tp} = 0.1$ km; 10 km), almost all TPs between 19 AU (10 AU; 27 AU) and the outer border of the considered region at 35 AU are spiralled inward. The two above mentioned concentrations obviously occur due to a stabilization effect of the action of several MMRs with Saturn, as well as with coinciding MMRs with Jupiter on the inward spiraling bodies. The stabilizing MMRs correspond to the semi-major axes in the intervals from 9 to 13 AU and from 15 to 18 AU (see Table 1).

In the region between the two concentrations of material, in the interval of distances ranging from about 13 AU to about 15 AU, the original material is gone. This is likely caused by the near 3:7 and 1:3 MMRs with Saturn.

The spiralling inward of the smallest considered objects with radii $R_{tp} = 0.1$ km (Fig. 1a) is interrupted only in the interval of heliocentric distances between 8 and 10 AU. This region of stability is obviously related to the 2:3, 3:4, 4:5, and, eventually, 5:6 MMRs with Saturn ($a = 9.6$, 8.8, 8.5, and 8.2 AU, respectively), and to 1:2 MMR with Jupiter ($a = 8.6$ AU). Eventually, the 2:5 and 3:7 MMRs with Jupiter ($a = 10.0$ and 9.5 AU) can be manifested, here.

The gas drag is not efficient on the larger bodies, having radii 100 and 1000 km in our simulation (Fig. 1d, e). Since no body spirals inward, the regions of the above mentioned mass concentration are not fed with mass, therefore the concentration of material is not increased above the initial level in any region beyond the Saturn's orbit.

If the dissipation of the nebula is relatively fast ($\tau = 1$ Myr), the bodies come into the regions of the active MMRs less frequently and, consequently, the measure of the concentration is lower (Fig. 1f) in this case. In run (f), the second mass-concentration peak occurs only in the interval of 17−18 AU and is only slightly rising above the initial state.

If the gas drag is permanently present and acting (Fig. 1g), the stabilization effect of the MMRs in the second mass-concentration region appears insufficient to compete with the drag driving deceleration of bodies and subsequent spiralling inward. The second, more distant accumulation of matter for an accretion of another ice-giant planet can, thus, appear only in the appropriately dissipating nebula. The checking run with no gas drag (Fig. 1h) only confirms that the drag force on large bodies can be neglected in the region beyond the orbit of Saturn (cf. Figs 1d, e and Fig. 1h).

3. The most probable sites of the accretion of Uranus and Neptune

In Fig. 1, we can see that the appearance of smaller ($R_{tp} \lessapprox 10$ km) objects increases in the regions of the active MMRs and the number of larger ($R_{tp} \gtrapprox 100$ km) ones is conserved in these regions (more exactly, beyond about 10 AU). All in all, these regions contain more matter at the end of the evolution than at its beginning. Thus, these regions seem to be the most appropriate sites in which another planets can form.

In this section, we attempt to specify the formation sites more precisely. Our result indicates the number of objects of various sizes in two regions of interest. Of course, a contribution of objects of a different size to the total mass is different. To characterize an accumulation of mass in an accretion region, we establish the *mid-plane mass surface density*, M_{mid}. In the analogy to the mid-plane number surface density, it is the mass inside the belt in the interval

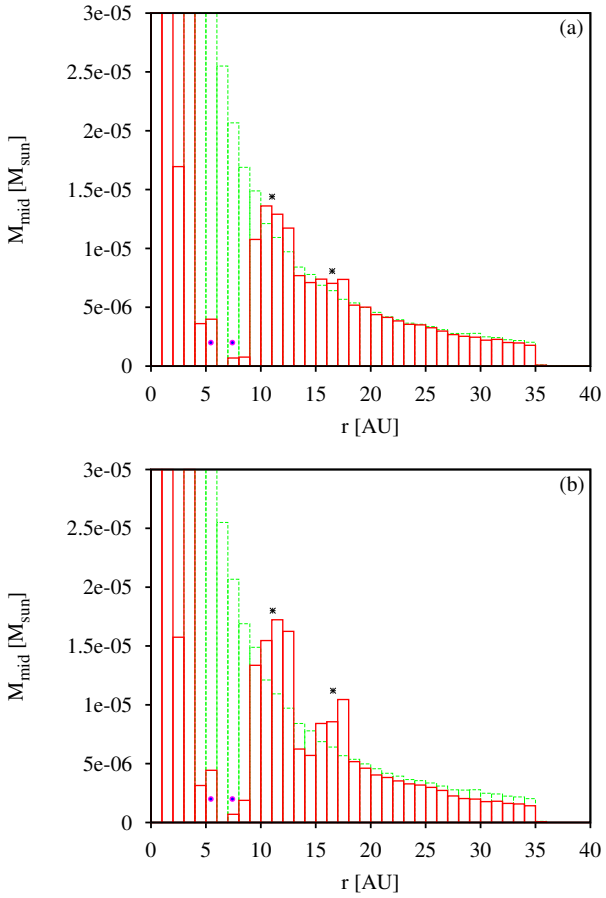

Figure 2. – 1-st part; figure continues on the next page.

of heliocentric distance from r to $r + dr$ and within the distance of 1 AU from the invariable or mid-plane of the planetary system.

The size (mean radius) differential distribution of the comet-sized as well as larger trans-Neptunian objects (TNOs) was found to be given in the form

$$n(R)\,dR = N_o R^{-s}\,dR, \tag{1}$$

where N_o is a normalization constant and s is the index of slope. Various authors have determined different values of s, from that lower than 3 to about 4.6 (Petit *et al.*, 2008, Table 3). If the small bodies had reached a collisional equilibrium, then $s = 3.5$ (Dohnanyi, 1969; see also Petit *et al.*, 2008). For $s > 4$, more and more mass is concentrated into smaller and smaller bodies (dust grains). In following, we would also like to demonstrate at least a rough dependence of

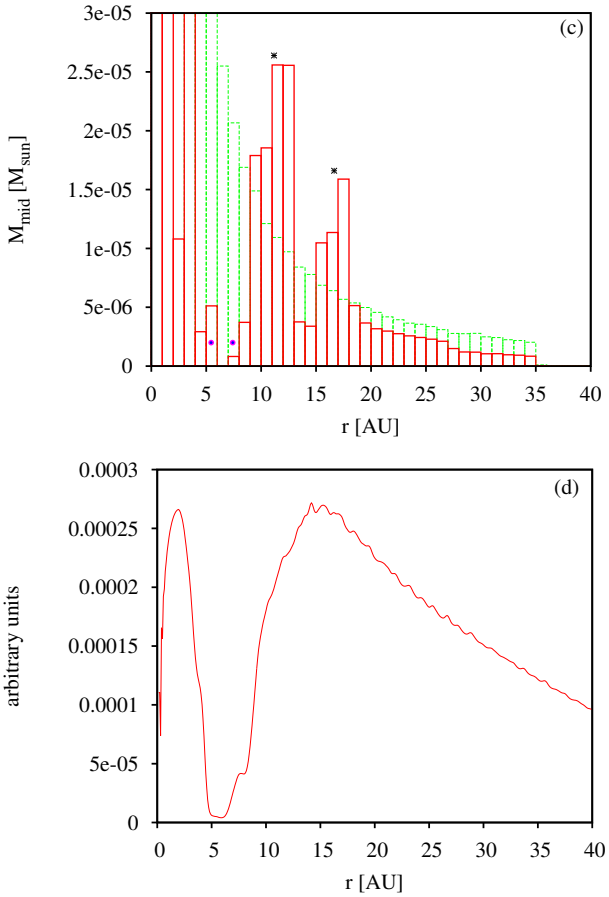

Figure 2. – 2-nd part; the 1-st part is on the previous page. The mid-plane mass surface density in 20 Myr (see Sect. 3 for details). Here, the integrated mass, M_{mid}, of the objects of all suitable sizes is summarized. The plots (a), (b), and (c) shows the density for the differential-distribution index $s = 3.7$, 4.0, and 4.3, respectively. Notice the different vertical scale of plot (c). The larger, violet (smaller, blue) full circles indicate the initial (final at 20 Myr) heliocentric distances of Jupiter and Saturn (on practically circular orbits) and black asterisks show the radii of circles representing the mass centres of the 2-AU-thick belts in the intervals of r from 9 to 13 AU and from 15 to 18 AU. Plot (d) shows the gas surface density profile taken from Morbidelli and Crida (2007).

the situation of Uranus and Neptune formations sites on the index, therefore we consider 3 values of the index: $s = 3.7$, 4.0, and 4.3. The lower value is supported by work of Tancredi et al. (2006), who found the index of the cumulative size distribution, s_c, for the Jupiter-family comets, which are supposed to originate in the scattering disc beyond Neptune and can be regarded as pristine bodies in the Solar System. According to Tancredi et al. (2006) $s_c = 2.7 \pm 0.3$, which corresponds to the differential index $s = 3.7$. The second value of $s = 4.0$ is chosen to demonstrate the case when the mass is distributed uniformly throughout the entire spectrum of objects' sizes. According to Jewitt et al. (1998) and Trujillo et al. (2001), this value is relevant for the TNOs. The last value of $s = 4.3$ is considered to simply keep the equidistant increment.

To determine the constant N_o, we take into account the fact that there are known two Pluto-sized ($R \gtrapprox 1000\,\mathrm{km}$) objects in the trans-Neptunian region. If we roughly assume a single such body per each 10 AU of the heliocentric distance in the range from 3 to 35 AU, i.e. 3 Pluto-sized objects, then this assumption will not, perhaps, be significantly contradicting to the abundance of the biggest objects beyond Neptune. The assumption yields $N_o = 3(1 - s)/1000^{1-s}$ (if the radii are given in kilometers).

In the case of $s = 3.7$, most of the mass is contained in the largest objects. However, the opposite is true for $s = 4.3$, therefore we need also to constrain the lower-end size border. Hughes (2001) studied the influx of long-period comets through the planetary region and found a significant lack of bodies fainter than the absolute magnitude $H = 6.6$. This absolute brightness corresponds, by Hughes' formula between H and the size of the body, to the mean radius of about 0.8 km. Hughes assumed that the large deviation of the long-period comet-size distribution from the power law (1) was caused by the discovery incompleteness. Analyzing the comet discoveries made by the LINEAR search programme, Francis (2005), however, demonstrated that the decrease of the number of faint comets is real. If we believe that the long-period comets originated in the once existing PPD, i.e. their today observed size distribution is consistent with the size distribution of small objects in the PPD, then we likely can ignore the bodies smaller than about 0.8 km at a mass inventory.

We note that a break in the law (1) was also found by Tancredi et al. (2006) for the Jupiter-family comets, which are known to come to the phase space of this cometary group from the trans-Neptunian region, i.e. the outer part of the PPD. Their size distribution should thus be consistent with the size distribution of the comet-sized objects in the PPD. Tancredi et al. (2006) found the break at the nuclear magnitude, defined by them, $H_N = 16.7$, which corresponds to the mean radius of 1.5 km for the albedo $\nu = 0.04$. Assuming a larger value of $\nu = 0.06$, for which Petit et al. (2008) argued, the break-point radius is something smaller, equal to about 1.2 km. Anyway, we can assume that there was not, obviously, much matter in the bodies with the radius smaller than $\sim$1 km, in the PPD.

There is one more reason that small bodies were not present in the PPD at the time, when the accretion of ice giants started. As seen in Fig. 1a, the small bodies are especially sensible to the gas drag and their radial motion inward is faster than that of larger bodies. We can suppose that they all fell onto the Sun, or were incorporated into the gas-giant planets, due to this fast spiralling, during the gas giants formation. Because of the above-mentioned reasons, we constrain the size distribution interval to bodies with the radius equal or larger than 1 km in our considerations.

In our simulation described in Sect. 2, we considered the TPs with radii, which can be identified with the centres of size-intervals from $10^{-1.5}$ to $10^{-0.5}$, then $10^{-0.5}$–$10^{0.5}$, $10^{0.5}$–$10^{1.5}$, $10^{1.5}$–$10^{2.5}$, and $10^{2.5}$–$10^{3.5}$ km. Denoting the lower border of the interval by R_{min} and upper border by R_{max}, the mass in the objects (TPs) with the radii in the given interval is

$$\begin{aligned} M_{min,max} &= \int_{R_{min}}^{R_{max}} n(R)m(R)\,dR = \\ &= \frac{4\pi\rho_{tp}N_o}{3(4-s)}\left(R_{max}^{4-s} - R_{min}^{4-s}\right) \qquad \text{if } s \neq 4, \\ &= \frac{4\pi}{3}\rho_{tp}N_o \ln\frac{R_{max}}{R_{min}} \qquad \text{for } s = 4, \end{aligned} \tag{2}$$

where we put $m(R) = 4\pi\rho_{tp}R^3/3$.

Starting with the size interval from $10^{-0.5}$–$10^{0.5}$ km, we can now easily calculate the mass distribution in the r-intervals of our interest, from 9 to 13 AU and from 15 to 18 AU (Fig. 1b, c). The corresponding distribution of the mid-plane mass surface density is shown in Fig. 2. If the mass is concentrated in large bodies (Fig. 2a), the regions of our interest are only slightly enriched with additional mass during the era of the solar-nebula dissipation. However, if more and more mass is concentrated to smaller, comet-sized bodies (Fig. 2b, c), the increase of the mass in these regions is significant. For example, it is roughly doubled for $s = 4.3$.

We can guess that another planets will accrete in the centres of the mass concentration in a given region. The radii of the mass centres are shown with asterisks in Fig. 2. More specifically, the radii are equal to 11.0 and 16.5 AU for $s = 3.7$, 11.1 and 16.6 AU for $s = 4.0$, and 11.2 and 16.6 AU for $s = 4.3$, i.e. they are practically insensitive to the distribution index, s, when the very small bodies are not considered.

Another reason of the accumulation of material in the 10–13 AU region (Fig. 2) can be following. The gas surface density profile taken from Morbidelli and Crida (2007), which we used, is shown in Fig. 2d. Notice that, at the outer edge of the gap opened by Jupiter and Saturn, where the surface density of that gas has a positive radial gradient, the gas has a super-keplerian rotation. This sets an additional trapping site, at the location where the gas changes from super-keplerian to sub-keplerian, i.e. where the surface density of the gas has

its maximum, outside the orbit of Saturn (around 15 AU). In the nearer-to-Sun region of a positive density radial gradient, between about 10 to 15 AU, the particles are forced to spiral outward. If there is a force, e.g. a resonance action, attempting to move them inward, the density gradient may balance this action and the particle can accumulate in the 10−15 AU interval. (In our simulation, the accumulation appears only in the 10−13 AU interval.) We need to keep in mind this effect as another possibility to accumulate the material.

In this section, we identified the most probable regions where giant planets could form. We found typically two maxima of solid material beyond the orbit of Saturn. In these regions, where the influence of the MMRs with Jupiter and Saturn as well as the trapping due to the positive density radial gradient on the first-hand side and the deceleration effect caused by gas drag on the other-hand side accumulated the material, the bigger object could grow. As an object grew there, it probably scattered the rest of material. This adverse-to-accumulation phenomenon is worth mentioning here, but the question of how much this effect reduces the accretion rate is beyond the scope of this paper.

4. Conclusion

The resonant action of Jupiter and Saturn in combination with the gas drag of dissipating solar nebula create two maxima in the distribution of solid material beyond the orbit of Saturn. Specifically, the distribution is peaked at about ~ 11 and ~ 16.5 AU. A higher amount of solid material is in smaller bodies (distribution index $s > 4$), the higher peaks occur. We suspect that the two maxima correspond to just two existing ice giants, Uranus and Neptune.

Namely, there are two principal concepts of the formation of these planets. According to the first, they occurred as a result of merging of many large, Mars-sized to Earth-sized, planetary embryos. According to the second concept, there formed only few (two) planetary embryos which grew up via an accretion of small planetesimals and dust. In this case, the embryos can be expected to form just in the regions of the maximum concentration of the solid material.

Acknowledgements. We thank Alessandro Morbidelli for a stimulating discussion and comments on our manuscript. This work was supported, in part, by VEGA - the Slovak Grant Agency for Science (grant No. 2/0031/14) and by the Slovak Research and Development Agency under contract No. APVV-0158-11.

References

Dohnanyi, J.S.: 1969, *J. Geophys. Res.* **74**, 2531
Duncan, M.J., Levison, H.F., Lee, M.H.: 1998, *Astron. J.* **116**, 2067
Francis, P.J.: 2005, *Astrophys. J.* **635**, 1348
Hayashi, C.: 1981, *Prog. Theor. Phys. Suppl.* **70**, 3
Jewitt, D.C., Luu, J.X., Trujillo, C.: 1998, *Astron. J.* **115**, 2125

Machida, M.N., Kokubo, E., Inutsuka, Sh.-I., Matsumoto, T.: 2010, *Mon. Not. R. Astron. Soc.* **405**, 1227
Masset, F., Snellgrove, M.: 2001, *Mon. Not. R. Astron. Soc.* **320**, L55
Morbidelli, A., Crida, A.: 2007, *Icarus* **191**, 158
Petit, J.-M., Kavelaars, J.J., Gladman, B., Loredo, T.: 2008, *Solar System beyond Neptune*, University of Arizona Press, Tucson, p. 71
Tancredi, G., Fernández, J.A., Rickman, H., Licandro, J.: 2006, *Icarus* **182**, 527
Trujillo, C.A., Jewitt, D.C., Luu, J.X.: 2001, *Astron. J.* **122**, 457
Tsiganis, K., Gomes, R., Morbidelli, A., Levison, H.F.: 2005, *Nature* **435**, 459